Clays and Clay Minerals, Vol. 43, No. 3, 337–345, 1995.

CHARACTERIZATION OF UNTREATED AND ALKYLAMMONIUM ION EXCHANGED ILLITE/SMECTITE BY HIGH RESOLUTION TRANSMISSION ELECTRON MICROSCOPY

KENAN CETIN* AND WARREN D. HUFF
Department of Geology, University of Cincinnati, Cincinnati, Ohio 45221

Abstract—High resolution transmission electron microscopy (HRTEM) have been performed on dispersed portions of one R > 1 and two R3 illite/smectite (I/S) samples from Silurian K-bentonites. R > 1 sample was studied by HRTEM before and after alkylammonium ion treatment and R3 samples were studied only after alkylammonium ion treatment. The HRTEM images of the chemically untreated R > 1 sample were predominated by lattice fringe contrast with 20–40 Å periods, interpreted to represent various ordered I/S units. HRTEM images of the three alkylammonium-treated samples displayed very small, dispersed particles composed of illite packets separated by alkylammonium expanded interlayers. In the R > 1 sample, illite packets were mostly 20 Å to 40 Å thick whereas in R3 samples they were predominantly over 40 Å. Although a good degree of dispersion of the bulk samples was achieved, dispersed particles recorded on images were thicker than the fundamental particles postulated by Nadeau and coworkers. Alkylammonium ion-expanded interlayer thicknesses point out a trend toward a higher charge in the expandable interlayers (i.e., illite particle surfaces) with increasing illite content from the R > 1 sample to the R3 samples. In the R3 samples, the interlayer charge is sufficiently high to be vermiculitic.

Key Words—Alkylammonium, Clays, Diagenesis, Illite, Interstratification, Smectite, Transmission Electron Microscopy.

INTRODUCTION

The structure of interstratified minerals, particularly that of illite/smectite (I/S), has been widely discussed (e.g., Nadeau *et al* 1984, 1985, Srodon *et al* 1986, Altaner and Bethke 1988, Eberl and Srodon 1988, Veblen *et al* 1990). Much of the recent interest in I/S stems from apparent discrepancies between the interpretation of I/S structure according to X-ray powder diffraction (XRD) and transmission electron microscope (TEM) data. Models of interstratification based on XRD (Reynolds 1980) suggest that I/S is composed of crystallites containing two types of layers, expanding smectite and non-expanding illite layers. XRD domain size considerations further suggest that I/S crystallites, also referred to as MacEwan crystallites (Altaner and Bethke 1988), are predominantly 5 to 15 2:1 layers thick. TEM observations, on the other hand, reveal that I/S, after being completely dispersed, is composed of extremely small particles, only one to a few silicate layers thick (Nadeau *et al* 1984, 1985, Nadeau 1985). Nadeau and coworkers termed these particles "fundamental particles" and interpreted them as primary particles rather than fragments of larger crystals. They further proposed that interparticle XRD effects between these particles account for what was generally interpreted as interstratification.

TEM, and in particular, high resolution transmission electron microscopy (HRTEM) has been the preferred analytical method of numerous workers attempting to resolve the discrepancies outlined above. Early HRTEM observations on dispersed or ion-thinned samples of I/S (e.g., Ahn and Peacor 1986, Bell 1986, Klimentidis and Mackinnon 1986, Vali and Köster 1986, Huff *et al* 1988) demonstrated the difficulty of differentiating a smectite layer from an illite layer and recognizing I/S ordering in electron microscopy observations. However, more recent computer simulations of electron microscopy images (Guthrie and Veblen 1989, 1990) have shown that under some special observation conditions illite and smectite layers and ordering can be recognized. These simulations have since enabled several workers to differentiate illite and smectite layers and to recognize their random or ordered interstratifications (Ahn and Peacor 1989, Veblen *et al* 1990, Jiang *et al* 1990). Ahn and Buseck (1990) and Veblen *et al* (1990) also showed that crystallites in I/S with coherent stacking relationships between 2:1 layers are usually thicker than the fundamental particles. They concluded that the smectite layers, being loosely bonded, are more easily cleaved than illite interlayers, and that the fundamental particles can be derived during sample preparation. This conclusion has been further substantiated by illite and smectite layer ratios in undisturbed samples as determined from HRTEM images that are consistent with those from XRD (Srodon *et al* 1990, Veblen *et al* 1990, Lindgreen and Hansen 1991).

* Present address: DataChem Laboratories, Glendale-Milford Road, Cincinnati, OH 45242.

Although most of the HRTEM data accumulated recently provide strong support for the existence of MacEwan crystallites in I/S clays whether or not the expanding interlayers in highly illitic, ordered I/S (or interfaces of fundamental illite particles) are smectitic remains poorly known and requires further attention. This paper reports HRTEM observations performed on dispersed portions of three, highly illitic, ordered I/S samples from K-bentonites, one chemically untreated and two others treated with alkylammonium chloride ions. The purpose of the study was to obtain high resolution structural information on the layer sequences and ordering of the samples as well as layer charge information by means of alkylammonium expanded interlayers. Alkylammonium ion treatment has been shown to provide a stable expansion of interlayers under HRTEM conditions (Rühlicke and Niederbudde 1985, Bell 1986, Klimentidis and Mackinnon 1986, Vali and Köster 1986, Marcks *et al* 1989, Ghabru *et al* 1989), even though it causes some disruption of the clay fabric (Lee and Peacor 1986). Furthermore, the type of structural arrangement adsorbed alkylammonium ions adopt can be inferred from the thickness of expanded interlayers on HRTEM images which, in turn, can be used to estimate the layer charge density of the expandable layers (Marcks *et al* 1989, Ghabru *et al* 1989, Olis *et al* 1990).

EXPERIMENTAL

Samples

Three highly illitic I/S samples from Silurian K-bentonites were selected for study by TEM. Chemical composition and XRD characteristics of these samples are described in detail by Cetin (1992) and Cetin and Huff (1994). Sample SI-47 has incomplete R2 (R = 1.5) ordering with about 83% illite layers. Since this sample has also been modeled as a mixture of R1 and R2 (R1/R2) or R1 and R3 (R1/R3) ordered I/S with around 77% illite layers, it will simply be referred to as sample R > 1 in the following discussion. According to XRD, both of the other two samples, WDH-68 and NI6, are long-range ordered (R3), and have 90% and 97% illite layers, respectively.

These samples were selected for TEM study because their <0.2 μm fractions are essentially pure I/S and they form a series of increasing illite content as well as an increasing degree of ordering, providing an opportunity to document the nature of different I/S ratios at high resolution. Also, the XRD characteristics of samples WDH-68 and NI6 indicate the presence of a segregated, vermiculite-like component when treated with long-chain alkylammonium chloride ions (Cetin 1992, Cetin and Huff 1994). HRTEM images of the alkylammonium-treated portions of these samples have the potential to show whether or not such segregated domains exist as structural entities.

Sample preparation

Samples for TEM were prepared by a technique modified from those of Vali and Köster (1986) and Marcks *et al* (1989). The technique is designed to minimize the formation of aggregates or clumps of sample material. In view of some studies that conclude that interstratification in I/S is merely an artifact due to aggregation of fundamental particles during XRD sample preparation (Nadeau *et al* 1984, 1985), an HRTEM study of I/S clays in a dispersed and aggregate-free system seems to be as important as, and complementary to, the HRTEM studies of I/S processed to preserve the original clay fabric (Ahn and Buseck 1990, Srodon *et al* 1990). An outline of the procedure is as follows: (1) The <0.2 μm fractions of the samples were obtained as overflow suspensions by centrifugation of coarse, Na-saturated bulk sample suspensions using a Sharples supercentrifuge. (2) Sample suspensions were then concentrated by repeated settling and decantation, and treated with long-chain alkylammonium ions: Sample R > 1 and one of the R3 samples (NI6) treated with hexadecylammonium chloride ions (Nc = 16, where Nc is the number of carbon atoms in the alkyl chain), and one R3 sample (WDH-68) with heptadecylammonium ions (Nc = 17). The alkylammonium treatment method follows essentially that of Rühlicke and Köhler (1981). (3) 20 to 30 mg of each alkylammonium-treated sample suspension was ultrasonically agitated for 1–2 minutes to ensure a homogeneous dispersion. (4) The ultrasonically-treated suspension was mixed in a ratio of about 1:5 by volume with epoxy resin (London-White) in a glass tube. The tube was closed with a stopper, and agitated for 1 minute in an ultrasonic bath, and then left at room temperature overnight. Because suspended particles settle to the lower half of the tube after about 12 hours, the resin/water mixture in the upper half was readily decanted and fresh resin added before another ultrasonic treatment. This procedure was repeated 2–3 times until water bubbles, indicating the presence of water in the mixture, were no longer detected following an ultrasonic treatment. In other words, ultrasonic treatment produces a homogeneous mixture of resin and suspended material provided little or no water is present. (5) About 5 ml of resin/sample suspension was poured into a mold and left to polymerize in an oven for 24 hours at 70°C. Polymerization was generally complete after about 15 hours. (6) The solid polymerized resin block was trimmed, and a pyramid tip was shaped (Figure 1). Ultrathin sections <500 Å thick were then cut from this pyramid shaped tip (Figure 1) by ultramicrotomy. (7) Ultrathin sections were mounted on nickel/copper TEM grids and carbon coated.

The technique described above differs from those of Vali and Köster (1986) and Marcks *et al* (1989) in that during the entire process dispersed clay particles were

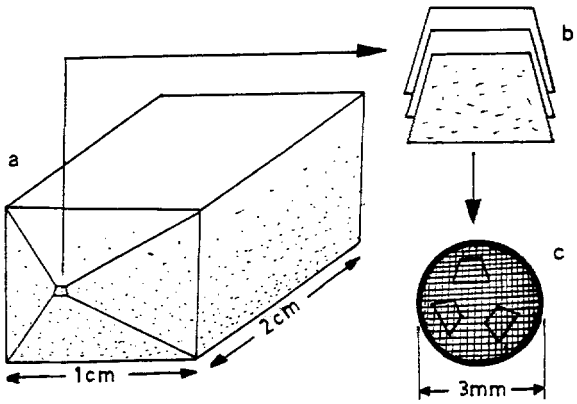

Figure 1. Trimmed resin block (a), and ultrathin microtome sections cut from the pyramid shaped tip before (b) and after mounting on a TEM grid (c).

not allowed to dry into aggregates. In addition, other techniques involve centrifugation of the resin/sample mold to obtain oriented aggregates of materials at the base of the resin block whereas the present technique maintains a good degree of dispersion of particles due to polimerization of resin synchronous with particle settling. Moreover, the ultrathin sections were cut from a part of the resin block (Figure 1) where particle concentrations are lower as compared to the base of the block where particles are more likely to form aggregates due to settling. The purpose in imaging dispersed particles by TEM as opposed to imaging a sample whose original fabric is preserved was to observe unambiguously whether or not the discrete clay particles are capable of intracrystalline expansion (i.e., interstratified) in a system principally identical to dispersed suspensions used in preparing XRD mounts.

Electron microscopy

Microtomed sections of the specimens were examined at 120 kV with a Philips CM20 transmission electron microscope having a structure resolution limit of about 2.6 Å (5.2 Å point-to-point resolution), and a spherical aberration coefficient (Cs) of 2.0 mm. Scherzer (optimum) defocus is approximately −1000 Å. A 50 μm objective aperture and a 100 μm condenser aperture were used for imaging.

Imaging was performed on numerous regions of ultrathin sections of each sample. Lattice fringe contrast consistent with I/S ordering was best observed at relatively large values of overfocus, a result consistent both with computer simulations and experimental studies (Guthrie and Veblen 1989, 1990, Veblen *et al* 1990, Jiang *et al* 1990). The extremely small size of particles on ultrathin sections, coupled with the high rate of beam damage, greatly impeded the recording of selected area diffraction (SAD) patterns; only a few could be obtained from rare large sample regions.

Numerous electron micrographs of several sample regions were obtained. Lattice fringe counts and measurements of crystallite thicknesses were made directly on image negatives by means of a Minolta RP605Z microfilm viewer with a magnification range of 13–27×.

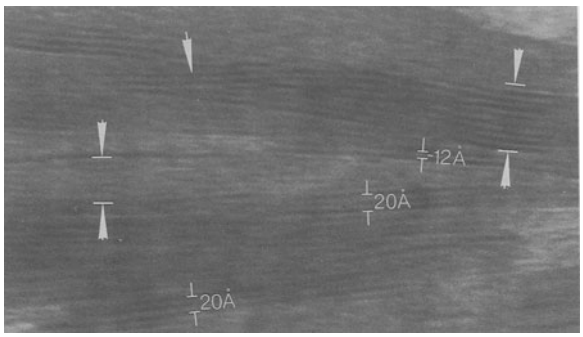

Figure 2. HRTEM image showing all three modes of occurrence of silicate layers observed in sample R > 1: 1) An illite packet (arrows on the left) consisting of six layers (number of interlayers + 1). The average periodicity of the dark fringes in the packet is 10 Å; 2) A smectite packet (arrows on the right) consisting of eight layers. The average periodicity of the dark fringes in the packet is about 12 Å; and 3) Two fairly obvious, ordered I/S units, each 20 Å thick. Also shown are a 12 Å silicate unit and a low-angle crystallite boundary (arrow on top).

RESULTS AND DISCUSSION

Untreated, dispersed R > 1 sample

Although a few wavy, sub-parallel and loosely-spaced aggregates of crystallites were observed in TEM images, the bulk of the R > 1 sample is represented by individual crystallites or particles that are mostly <1000 Å in their longest dimension. Thus, imaging of these crystallites required HRTEM magnification for details of their extremely fine structure. Some representative lattice fringe images of sample R > 1 are shown in Figures 2 and 3.

Figure 2 is unique because it is the only image that displays the three principal modes of lattice fringes observed in the R > 1 sample. First, packets, composed of straight, light fringes alternating with thin, dark fringes with an average periodicity of 10 Å, which are interpreted to be illite (Figure 2). These packets are usually observed to have more than four light fringes. Second, packets, composed of somewhat wavy, light fringes alternating with heavier dark fringes with an average periodicity of about 12 Å, which are interpreted to be partially collapsed smectite (Figure 2). This feature was observed in only two images. Third, 20 Å, 30 Å, or 40 Å thick units, composed of 10 Å illite fringes bordered by heavier dark fringes that are identical to smectite fringes (Figures 2, 3a and 3b). These sets of lattice fringe units are interpreted to have resulted from I/S ordering.

https://doi.org/10.1346/CCMN.1995.0430308 Published online by Cambridge University Press

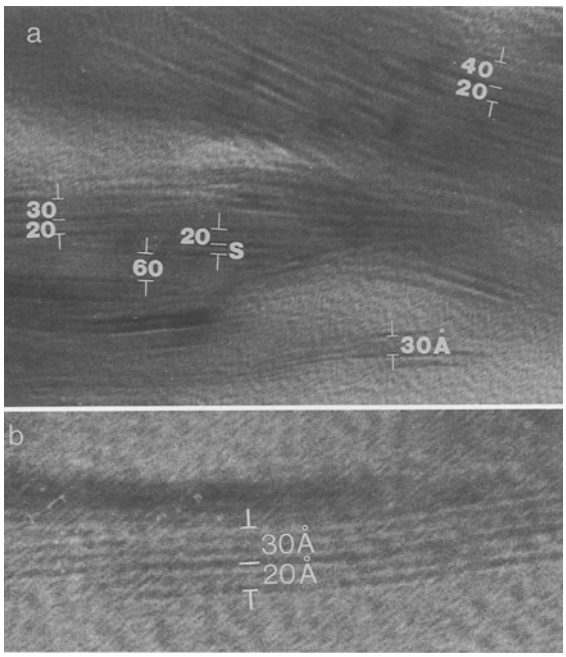

Figure 3. Two HRTEM images from sample R > 1. (a) An image showing lattice fringe units of 20 Å, 30 Å and 40 Å thickness, a single layer unit (S), and a 60 Å thick packet of illite layers. (b) Enlargement of a region near the lower left corner of (a) showing adjacent 20 Å and 30 Å units not apparent in (a).

The interpretations of lattice fringes described above are consistent with computer simulations of Guthrie and Veblen (1989, 1990) who showed that less intense dark fringes correspond to illite interlayers while heavier dark fringes correspond to smectite interlayers. Most of the imaged sample regions in the R > 1 sample are composed of mixtures of ordered I/S units similar to those shown in Figures 3a and 3b. Therefore, sample R > 1 does not appear to consist of perfectly ordered illite and smectite layers, which is supported by XRD characteristics of the sample.

In addition to basal lattice fringes arising from 001 reflections, some images display areas with 4.5 Å cross-fringes (Figure 4) formed by hkl reflections. These fringes seem to have formed in regions of warped or twisted crystallites which were slightly underfocused. Most of the cross-fringes extend across 3–5 silicate layers and some extend well across ten silicate layers. Computer-simulated intensity profiles and experimental results (Veblen *et al* 1990) demonstrated that 4.5 Å cross-fringes are strong indicators of coherent (i.e., non-turbostatic) stacking of adjacent 2:1 layers over the regions they traverse.

Alkylammonium ion-treated, dispersed I/S

XRD patterns of the samples treated with long-chain alkylammonium chloride ions show a low-angle reflection at about 30 Å (Figure 5). In the case of the R > 1 sample, this reflection appeared to have resulted from the expansion of smectite-like charged interlayers due to a bilayer/pseudotrimolecular arrangement of alkylammonium ions. Similar reflections observed for both R3 samples, however, were attributed to a paraffin-type arrangement of alkylammonium ions that expanded the interlayers of a vermiculite-like charged component (Cetin 1992). Comparison of the XRD and TEM data is addressed below.

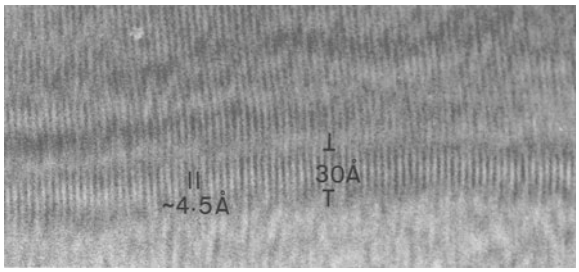

Figure 4. Enlargement of a HRTEM image showing cross-fringes with 4.5 Å periods on a crystallite edge in the R > 1 sample. The area in the upper part of the image exhibiting cross-fringes is more than 100 Å thick. Faint outline of a 30 Å period shows the roughly horizontal basal fringes.

Ultrathin sections of the alkylammonium-treated samples are dominated by extremely small, isolated particles, mostly several hundred angstroms thick parallel to the c*-axis, indicating a good degree of dispersion. On the other hand, no area recorded on the images obtained from alkylammonium-treated samples shows a 10 Å lattice fringe periodicity typical of illite (e.g., Figures 2 and 3). Several attempts using various crystal orientation and microscope focus conditions were made but they failed to produce a 10 Å periodicity. However, images obtained near or at Scherzer focus displayed packets of dark fringes that were consistently integral multiples of 10 Å in thickness (i.e., 30 Å, 40 Å, etc.). The packets of dark fringes were separated by light fringes variable in thickness. Scherzer-focused images usually have a "normal" contrast where dark fringes overlay areas of high charge density, and bright fringes overlay areas of low charge density. Such images portray accurate structural information (Guthrie and Veblen 1990). In the images presented below determined to have a normal contrast (Figures 6–9), we concluded that dark fringes that are integral multiples of 10 Å represent illite packets and the light fringes represent alkylammonium-expanded interlayers. The uneven spacing and variable thickness of the light fringes have been used as the main criteria to distinguish if an image had normal contrast. Individual packets of dark fringes were measured from one edge of the other along the apparent c*-axis. Thickness of an interlayer area was determined by subtracting the thicknesses of two adjacent packets from the total measured thickness. Less intact crystallite edges were avoided in measurements.

https://doi.org/10.1346/CCMN.1995.0430308 Published online by Cambridge University Press

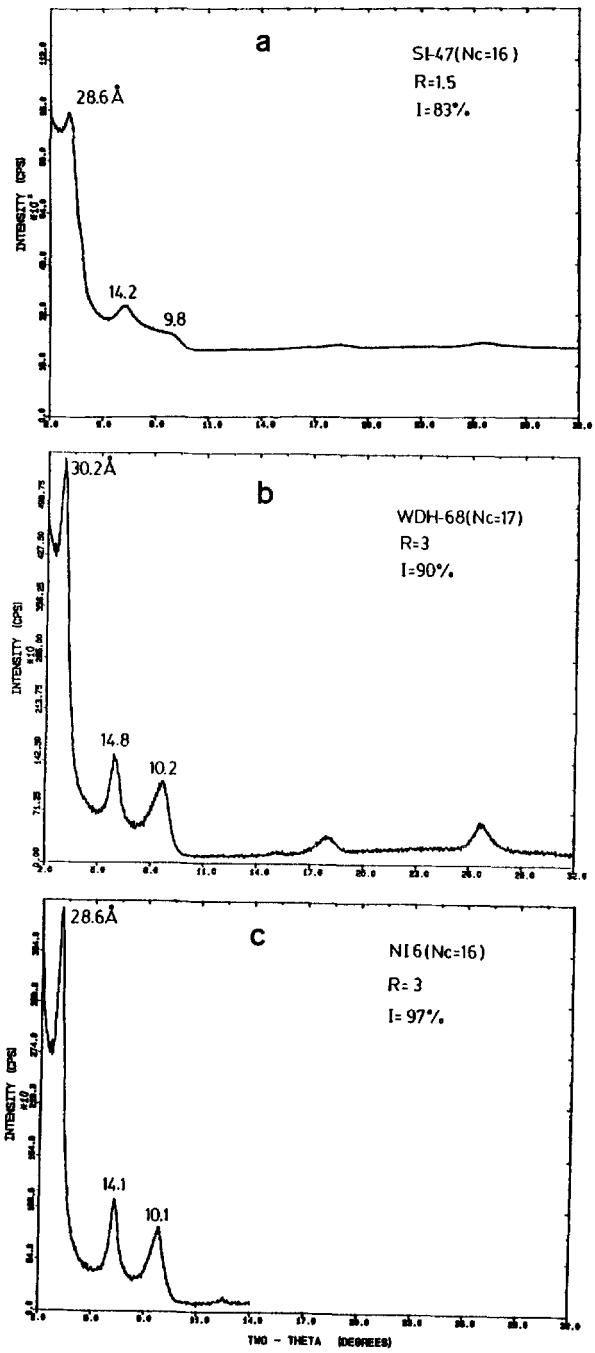

Figure 5. XRD patterns of samples after alkylammonium ion treatment. (a) R > 1 ordered sample (SI-47) treated with hexadecylammonium chloride ions. (b) R3 ordered sample (WDH-68) treated with heptadecylammonium ions; c) R3 ordered sample (NI6) treated with hexadecylammonium ions.

R > 1 sample. The general results concerning the alkylammonium-treated R > 1 sample are illustrated with two representative images (Figures 6 and 7). Figure 6 shows a relatively low-magnification image of

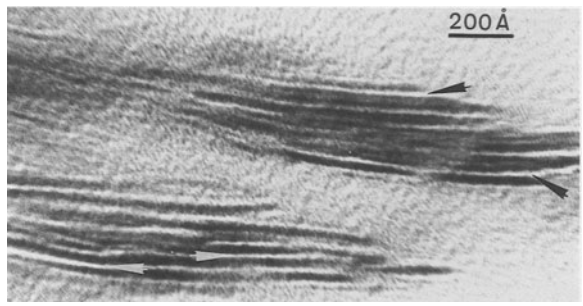

Figure 6. HRTEM image of hexadecylammonium chloride-treated R > 1 sample showing expanded interlayers (arrowed light fringes) and clay packets, presumably of illite, which the two particles are composed of.

two clay particles that are 300–350 Å thick parallel to the crystallographic c*-axis. Figure 7 shows an enlarged image that illustrates the tendency of particles similar to the ones shown in Figure 6 to separate into smaller packets, presumably of illite, that are mostly 30 Å or 40 Å thick from one edge to the other (Figure 7). However, discrete illite packets, 20 Å, 30 Å or 40 Å thick, were not observed in any of the ultrathin sections examined. Higher magnification images and enlargements of low-magnification images reveal that the light fringes which define packet boundaries within larger crystallites or particles do indeed represent alkylammonium expanded interlayers. They are mostly 15–16 Å thick in more stable crystallite interiors (e.g., Figure 7) and tend to be thicker near crystallite edges.

The 28.6 Å reflection in the XRD pattern of the alkylammonium-treated R > 1 sample (Figure 5a) suggests the presence of a segregated component of similar periodicity. TEM images of the R > 1 sample, however, do not display any segregated packets with expanded interlayers in sample regions recorded on images. This discrepancy between the XRD results and the HRTEM observations is probably due to a combination of: 1) small volume in the bulk sample of the segregated and expandable component that produced the 29 Å reflection on the XRD pattern and the few packets of smectite-like layers observed in this sample prior to alkylammonium treatment (e.g., Figure 2); and 2) very small sample sizes characteristic of HRTEM studies that may preclude observation of features inferred from XRD.

R3 ordered samples. HRTEM images of two, R3 ordered samples treated with alkylammonium ions are generally similar to those of the alkylammonium-treated R > 1 sample. However, the R3 samples do have several characteristics which differ from the R > 1 sample. First, the measured illite packets, mostly over 40 Å, are predominantly thicker than those of the R > 1 sample. These packets are apparently parallel-oriented and somewhat coherently stacked, although

https://doi.org/10.1346/CCMN.1995.0430308 Published online by Cambridge University Press

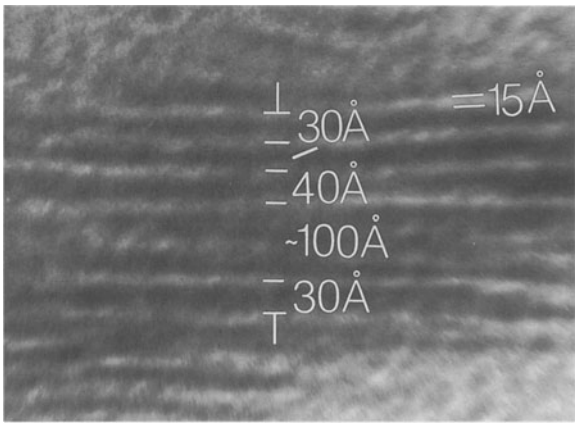

Figure 7. HRTEM image of a crystallite showing measured illite packet and expanded interlayer thicknesses in hexadecylammonium chloride-treated R > 1 sample.

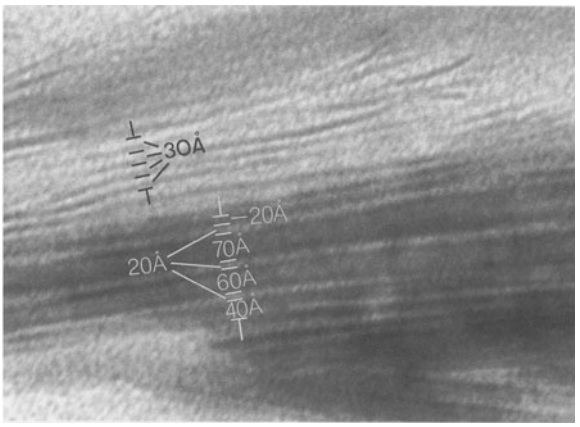

Figure 9. HRTEM image of heptadecylammonium-treated R3 sample (WDH-68) showing a region with 30 Å lattice fringe periodicity adjacent to a region of illite packets separated by 20 Å thick expanded interlayers.

some pinch out or terminate (Figure 8). Second, alkylammonium expanded interlayers are less variable in thickness, with a spacing of approximately 20 Å, suggesting a more homogeneous charge density in the interlayers. Expanded interlayers >20 Å are also observed (Figure 8). Finally, several images of the R3 samples display a 30 Å expanded-layer periodicity in relatively large sample areas (e.g., Figure 9). These 30 Å periods consist of 20 Å light fringes representing expanded interlayers alternating with 10 Å dark fringes representing single silicate layers.

Interpretation of HRTEM images and their implications for the structure of illitic I/S

HRTEM images of the sample R > 1 are dominated by crystallites, parts of which display 20 Å, 30 Å, and 40 Å lattice fringe contrast. These units of lattice fringe contrast (Figures 2 and 3) were recognized as ordered illite and smectite layers, based on couplets, triplets or quadruplets of light fringes representing illite alternating with thin dark fringes (corresponding approximately to illite interlayers), which were bounded by heavier dark fringes (corresponding approximately to smectite interlayers). This interpretation is in accordance with computer simulation results of Guthrie and Veblen (1989, 1990) and thus, such units are considered to represent parts of ordered I/S sequences in the R > 1 sample. Lattice fringe contrast consistent with ordering of I/S units described above are exhibited only in parts of the images and repeats of adjacent units along the apparent stacking direction occur only for very short distances (e.g., Figure 3b). The general lack of extended areas with described lattice fringe contrast may be attributable to the variable orientation of the silicate layers in the third dimension relative to the electron beam direction. The orientation of layers is critical since image modulations indicative of ordering of illite and smectite layers (e.g., 20 Å periodicity) are shown to be best observed when the layers are slightly tilted with respect to the incident beam (Veblen *et al* 1990). The very small size of the clay particles, which makes tilting difficult, and the sensitivity of the particles to the electron beam were also responsible for the apparent absence of larger areas with lattice fringe contrast indicative of I/S ordering.

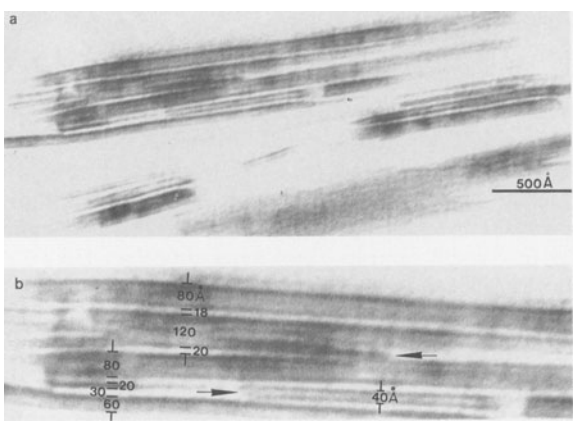

Figure 8. Two HRTEM images of heptadeclyammonium chloride-treated R3 sample (WDH-68) (a) an image showing dispersed crystallites that contain expanded interlayers. (b) Enlargement of part of (a) showing the thickness of illite packets and expanded interlayers. Note irregularities in the stacking such as subparallelism or termination of packets (shown by arrows).

Although the interpretation of the observed 20 Å and 30 Å periods is consistent with lattice fringe contrast due to I/S ordering, there are two other possible interpretations. The first possibility is that lattice fringes with 20 Å and 30 Å periodicities may also result from polytypic periodicities in 2M and 3T mica polytypes, respectively (Iijima and Buseck 1978, Guthrie

https://doi.org/10.1346/CCMN.1995.0430308 Published online by Cambridge University Press

and Veblen 1989). However, it is difficult to attribute the presence of these periodicities to polytypes in the absence of evidence for 2M and 3T polytypes from XRD data (Cetin 1992).

The second possibility is that lattice fringes with 20–40 Å periodicities in the R > 1 sample or the measured packets of similar thicknesses in alkylammonium-treated samples may be due to stacked "fundamental illite particles" (Nadeau *et al* 1984, 1985). However, several images containing 4.5 Å cross-fringes (Figure 4) suggest that the range of coherent stacking across silicate layers in the R > 1 sample is invariably larger than the illite particle thicknesses observed in I/S of similar composition (see particle distributions in Nadeau *et al* 1985). This observation is in agreement with the recent studies of Ahn and Buseck (1990) and Veblen *et al* (1990) which also indicated that the range of coherently stacked 2:1 layers exceeds the size of fundamental particles. Furthermore, the longest dimension of most crystallites observed on images from all three alkylammonium-treated samples is <1000 Å, significantly smaller than the average particle lengths in highly illitic, completely dispersed I/S samples (about 3000 Å; Table 2; Nadeau 1985). This suggests that the degree of dispersion achieved in the present samples is excellent. Despite this, however, discrete particles similar in thickness to the fundamental particles reported for highly illitic I/S (50–90 Å thick; Nadeau 1985) are not observed. Instead, dispersed particles appear to consist of several packets similar in thickness to the fundamental illite particles (Figures 6–9). Therefore, the apparent coherent stacking and c*-axis thicknesses of the well-dispersed particles observed in this study, coupled with their intraparticle expansion behavior, strongly suggest that they are produced by disintegration of larger crystallites.

It should be noted that particles that might have loosely aggregated during sample preparation or that are aggregated because they did not fully disintegrate during dispersion were largely excluded from our TEM observations (since microtomed sections were selected from regions of lower particle concentration). It is conceivable that those portions of the samples contain larger crystallites with intracrystalline expansion behavior as well, which may better represent the true crystallite dimensions in the bulk, undisturbed bentonite rock. A comprehensive characterization of the true crystallite dimensions in illite-rich I/S, especially their c*-axis thicknesses, requires further examination using tools of direct observation such as TEM in samples processed to retain the original rock fabric.

Layer charge density as inferred from alkylammonium expanded interlayer thicknesses on HRTEM images

The alkylammonium ions absorbed into the expanding interlayers of 2:1 layer silicates can be arranged in monolayers (≈4 Å), bilayers (≈8 Å), pseudotrimolecular layers (≈8–18 Å) and paraffin type structures (12–25 Å) (Lagaly and Weiss 1969, 1976). Lagaly and coworkers showed that adsorption of alkylammonium ions by 2:1 expanding silicates proceeds by a cation exchange reaction, which led to the development of the alkylammonium ion exchange method. This method allows both the magnitude and the distribution of layer charge density to be determined using the relationship between the type of alkylammonium arrangement as inferred by XRD basal spacings and the alkylammonium chain length. An extensive determination of the distribution of layer charge in bulk 2:1 expanding clays requires preparation of complexes from several alkylammonium ions. Also, though less precise, a rapid and practical method of estimation of layer charges using an XRD basal spacing from a single alkylammonium expansion has recently been introduced (Olis *et al* 1990). On the other hand, a practical estimation of the range of layer charge density is also possible by inferring the type of alkylammonium arrangement from expanded interlayer thicknesses on HRTEM images. Several recent HRTEM studies have indeed proven the utility of such a technique by confirming the XRD basal spacings observed for monomineralic smectite and vermiculite on high resolution images (Vali and Köster 1986, Rühlicke and Niederbudde 1985, Ghabru *et al* 1989, Marcks *et al* 1989). In the present study, hexadecylammonium (Nc = 16) and heptadecylammonium (Nc = 17) ions have been used to form expanded complexes of I/S. Therefore, both XRD and HRTEM spacings from the previous studies that have been obtained for the long-chain alkylammonium (Nc = 16–18) complexes of smectites and vermiculites have been utilized to serve as guidelines.

As noted earlier, images obtained near or at Scherzer focus and having a normal contrast were used in the measurement of alkylammonium expanded interlayer thicknesses. Tens of measurements on the images of the R > 1 sample show that the expanded interlayers between the illite packets are predominantly 15–16 Å thick in more intact crystallite interiors, indicating a monolayer-to-bilayer arrangement of alkylammonium ions. Such transitional arrangements with hexadecylammonium ions (Nc = 16) have previously been observed for natural high-charge smectite (0.45–0.60) as well as low-charge vermiculite (0.60–0.70) samples (Lagaly and Weiss 1976, Lagaly 1982). Thus, whether the expanded interlayer thicknesses of 15–16 Å represent a smectitic or a vermiculitic layer charge density cannot be assessed with certainty. Cetin and Huff (1994) have shown that the R > 1 sample has a smectitic charge in the range 0.36–0.51 using the conventional alkylammonium ion exchange. It is plausible that the conventional method gives a better approximation of the interlayer charge because of the use of XRD basal spacings than comparatively low number of interlayer thickness measurements available from TEM images.

At any rate, the R > 1 sample may be regarded to possess a high-charge smectitic to a low-charge vermiculitic charge density.

On the other hand, the expanded interlayers between the illite packets of the two R3 samples are predominantly 20 Å or thicker, strongly suggesting the presence of pseudotrimolecular to paraffin-type structures observed in several high-charge (>0.7) vermiculite samples (Lagaly 1981, Ghabru *et al* 1989, Marcks *et al* 1989). Relatively uniform interlayer thicknesses exhibited by these two samples are also consistent with more homogeneous interlayer charge distribution typical of high-charge vermiculite samples.

Treating the R3 samples with hexadecylammonium (Nc = 16) and heptadecylammonium (Nc = 17) ions revealed no smectite-like expanding interlayers. This is in contrast to the observations by Vali *et al* (1991), who identified a smectite-like expanding component in highly illitic materials treated with octadecylammonium ions (Nc = 18), in addition to a vermiculite-like expanding component and non-expanding illite. The observation in the R3 samples of areas with a 30 Å lattice fringe periodicity supports the XRD data which suggested the presence of a segregated vermiculite-like component (Figures 5b and 5c). However, Laird *et al* (1987) presented an alternative explanation for the presence of this segregated, vermiculite-like charged component that they may be illite interlayers expanded because of an exchange reaction between alkylammonium ions and K^+. Considering that present models of the I/S structure do not predict even small volumes of a segregated and expandable component (e.g., Reynolds 1980, Nadeau *et al* 1985, Altaner and Bethke 1988), the segregated domains observed in our TEM images may indeed be expanded illite interlayers. Nonetheless, the present observations of increased alkylammonium-expanded interlayer thicknesses point out a trend toward a higher layer charge of expandable interlayers (i.e., illite particle surfaces) with increasing illite content from the R > 1 sample to the R3 samples. In the R3 samples, the interlayer charge is sufficiently high to be termed vermiculite.

ACKNOWLEDGMENTS

This research was supported, in part, by NSF grants EAR-89004295 and INT-8419409 to W. D. Huff, and by a Clay Minerals Society Student Research Grant to K. Cetin. The paper benefited greatly from a thorough review by an anonymous reviewer, as well as from comments by G. Lagaly. Improvements to the language of the text by Tammie Gerke are greatly appreciated.

REFERENCES

Ahn, J. H., and P. R. Buseck. 1990. Layer-stacking sequences and structural disorder in mixed-layer illite/smectite: Image simulations and HRTEM imaging. *Amer. Mineral.* **75**: 267–275.

Ahn, J. H., and D. R. Peacor. 1986. Transmission and analytical electron microscopy of the smectite-to-illite transition. *Clays & Clay Miner.* **34**: 165–179.

Altaner, S. P., and C. M. Bethke. 1988. Interlayer order in illite/smectite. *Amer. Mineral.* **73**: 766–774.

Ahn, J. H., and D. R. Peacor. 1989. Illite/smectite from Gulf Coast shales: A reappraisal of transmission electron microscope images. *Clays & Clay Miner.* **37**: 542–546.

Bell, T. E. 1986. Microstructure in mixed-layer illite/smectite and its relationship to the reaction of smectite to illite. *Clays & Clay Miner.* **34**: 146–154.

Cetin, K. 1992. The Nature of Illite/Smectite Clays and Smectite Illitization in Paleozoic K-bentonites. Ph.D. dissertation. University of Cincinnati, Cincinnati, Ohio, 200 pp.

Cetin, K., and W. D. Huff. 1995. Layer charge of the expandable component of illite/smectite in K-bentonite as determined by alkylammonium ion exchange. *Clays & Clay Miner.* (in press).

Eberl, D. D., and J. Srodon. 1988. Ostwald ripening and interparticle-diffraction effects for illite crystals. *Amer. Miner.* **43**: 1335–1345.

Ghabru, S. K., A. Mermut, and R. J. S. Arnaud. 1989. Layer charge and cation-exchange characteristics of vermiculite (weathered biotite) isolated from a gray luvisol in northeastern Saskatchewan. *Clays & Clay Miner.* **37**: 164–172.

Guthrie, G. D., and D. R. Veblen. 1989. High-resolution transmission electron microscopy of mixed-layer illite/smectite: Computer simulations. *Clays & Clay Miner.* **37**: 1–11.

Guthrie, G. D., and D. R. Veblen. 1990. Interpreting one-dimensional high-resolution transmission electron micrographs of sheet silicates by computer simulation. *Amer. Mineral.* **75**: 276–288.

Huff, W. D., J. A. Whiteman, and C. D. Curtis. 1988. Investigation of a K-bentonite by x-ray diffraction and analytical electron microscopy. *Clays & Clay Miner.* **36**: 83–93.

Iijima, S., and P. R. Buseck. 1978. Experimental study of disordered mica structures by high-resolution electron microscopy. *Acta Crystallogr.* **A34**: 709–719.

Jiang, W. T., D. R. Peacor, R. J. Merriman, and B. Roberts. 1990. Transmission and analytical electron microscopic study of mixed-layer illite/smectite formed as a replacement of diagenetic illite. *Clays & Clay Miner.* **38**: 449–468.

Klimentidis, R. E., and I. D. R. Mackinnon. 1986. High-resolution imaging of ordered mixed-layer clays. *Clays & Clay Miner.* **34**: 155–164.

Lagaly, G. 1981. Characterization of clays by organic compounds. *Clay Miner.* **16**: 1–21.

Lagaly, G. 1982. Layer charge heterogeneity in vermiculites. *Clays & Clay Miner.* **30**: 215–222.

Lagaly, G., and A. Weiss. 1969. Determination of layer charge in mica-type layer silicates. Proceedings of the International Clay Conference, Tokyo, Japan. L. Heller, ed., 61–80.

Lagaly, G., and A. Weiss. 1976. The layer charge of smectitic layer silicates. Proceedings of the International Clay Conference, Mexico City, Mexico, 1975, 157–172.

Laird, D. A., A. D. Scott, and T. E. Fenton. 1987. Interpretation of alkylammonium characterizations of soil clays. *Soil Sci. Soc. Am. J.* **51**: 1659–1663.

Lee, J. H., and D. R. Peacor. 1986. Expansion of smectite by laurylamine hydrochloride: Ambiguities in transmission electron microscopy results. *Clays & Clay Miner.* **34**: 69–73.

Lindgreen, H., and P. L. Hansen. 1991. Ordering of illite-smectite in upper Jurassic claystones from the North Sea. *Clay Miner.* **26**: 105–125.

Marcks, CH., H. Wachsmuth, and H. G. V. Reichenbach. 1989. Preparation of vermiculites for HRTEM. *Clay Miner.* **24**: 23–32.

Nadeau, P. H. 1985. The physical dimensions of fundamental clay particles. *Clay Miner.* **20**: 499–514.

Nadeau, P. H., J. M. Tait, W. J. McHardy, and M. J. Wilson. 1984. Interstratified XRD characteristics of physical mixtures of elementary clay particles. *Clay Miner.* **19**: 67–76.

Nadeau, P. H., M. J. Wilson, W. J. MacHardy, and J. M. Tait. 1985. The conversion of smectite to illite during diagenesis: Evidence from some illitic clays from bentonites and sandstones. *Mineralog. Maga.* **49**: 393–400.

Olis, A. C., D. B. Malla, and L. A. Douglas. 1990. The rapid estimation of the layer charges of 2:1 expanding clays from a single alkylammonium ion expansion. *Clay Miner.* **25**: 39–50.

Reynolds, R. C., Jr. 1980. Interstratified clay minerals. In *Crystal Structure of Clay Minerals and their X-ray Identification.* G. W. Brown and G. Brown, eds. London: Mineralogical Society, 249–303.

Rühlicke, G., and E. E. Köhler. 1981. A simplified procedure for determining layer charge by the n-alkylammonium method. *Clay Miner.* **16**: 305–307.

Rühlicke, G., and E. A. Niederbudde. 1985. Determination of layer-charge density of expandable 2:1 clay minerals in soils and loess sediments using the alkylammonium method. *Clay Miner.* **20**: 291–300.

Srodon, J., D. J. Morgan, E. Eslinger, D. D. Eberl, and M. R. Karlinger. 1986. Chemistry of illite/smectite and end-member illite. *Clays & Clay Miner.* **34**: 368–378.

Srodon, J., C. Andreoli, F. Elsass, and M. Robert. 1990. Direct high-resolution transmission electron microscopic measurement of expandability of mixed-layer illite/smectite in bentonite rock. *Clays & Clay Miner.* **38**: 373–379.

Vali, H., and H. M. Köster. 1986. Expanding behavior, structural disorder, regular and random irregular interstratification of 2:1 layer silicates studied by high-resolution images of transmission electron microscopy. *Clay Miner.* **21**: 827–859.

Vali, H., R. Hesse, and E. E. Köhler. 1991. Combined freeze-etched replicas and HRTEM images as tools to study fundamental-particles and multi-phase nature of 2:1 layer silicates. *Amer. Mineral.* **76**: 1953–1964.

Veblen, D. R., G. D. Guthrie, J. T. L. Kenneth, Jr., and R. C. Reynolds, Jr. 1990. High-resolution transmission electron microscopy and electron diffraction of mixed-layer illite/smectite: Experimental results. *Clays & Clay Miner.* **38**: 1–13.

(Received 4 January 1994; accepted 7 November 1994; Ms. 2449)